Current Research in Microbial Sciences 8 (2025) 100379

Contents lists available at ScienceDirect

Current Research in Microbial Sciences

journal homepage: www.sciencedirect.com/journal/current-research-in-microbial-sciences

Impact of *Pseudomonas aeruginosa* biofilm formation by different sequence types on treating lower limb vascular infections

Yudi Wang [a,b,1], Qian Xiao [b,1], Qiong Yang [b,c,1], Yulin Long [a,b], Zhibiao Jiang [b], Tantao Zhang [b], Ying Hu [b], Bingru Gao [d], Xuanyu Chen [d], Ting Wang [e,*], Linlin Xiao [b,a,c,*]

[a] Southern Medical University, Guangdong, 510515, China
[b] Shanghai Fengxian District Central Hospital, Shanghai, 201499, China
[c] Jinzhou Medical University, Liaoning, 121001, China
[d] School of Health Science and Engineering, University of Shanghai for Science and Technology, Shanghai, 200093, China
[e] Shanghai Urban Construction Vocational College, Shanghai, 201415, China

ARTICLE INFO

Keywords:
Pseudomonas aeruginosa
Multidrug resistance
Biofilm
Virulence genes
Antimicrobial resistance genes

ABSTRACT

Pseudomonas aeruginosa is a major contributor to persistent chronic infections in clinical practice, owing to its robust biofilm formation capacity and frequent antimicrobial resistance acquisition. However, most current studies focus on single strains and thus overlook phenotypic differences among coexisting strains within the same host. With that in mind, we proposed a hypothesis that *P. aeruginosa* strains from the same patient, yet with distinct genetic backgrounds, might exhibit differing resistance profiles and virulence genes. To test this hypothesis, we selected three strains with different sequence types (STs), all isolated from the chronic wounds of a patient with long-term bilateral lower limb infections. By employing multilocus sequence typing, antimicrobial susceptibility testing, biofilm gene quantification, growth kinetics assays, Galleria mellonella virulence experiments, and phylogenetic reconstruction, we systematically evaluated the relationships between these strains'-biofilm formation and virulence. The results revealed significant genetic diversity and evolutionary origin variations among the three strains. Notably, ST2584 (WYDPA-23-3) exhibited multidrug resistance (resistant to 7 of the 12 tested antibiotics) and the highest growth rate, whereas ST270 (WYDPA-23-2)—despite the down-regulation of *pelA*, a gene linked to extracellular matrix biogenesis—demonstrated a 2.3-fold increase in biofilm formation and the highest larval lethality. By comparing multiple strains coexisting in the same host, this study further elucidates the role of *P. aeruginosa* biofilm in sustaining chronic infections and offers valuable guidance for optimizing clinical treatment strategies and antibiotic selection. In light of these findings, developing rapid and precise biofilm detection methods and designing innovative drugs targeting high biofilm-producing strains should be prioritized.

1. Introduction

Pseudomonas aeruginosa is a leading pathogen in nosocomial infections worldwide, exhibiting significant specificity in infection types and population distribution (Boustanshenas et al., 2023). According to the latest data from the 2025 Global Antimicrobial Resistance Surveillance System (GLASS) report, *P. aeruginosa* predominates in chronic lower limb infections (34.8 %), burn wound infections (31.2 %), and ventilator-associated pneumonia (18.6 %) (Brzozowski et al., 2020). In different infection scenarios, *P. aeruginosa* establishes unique pathogenic niches by dynamically regulating virulence factors and immune evasion strategies (Bogiel et al., 2023). Moreover, biofilm formation and its regulatory network are central drivers of escalating antibiotic resistance and the persistence of chronic infections (Pusic et al., 2021).

The biofilm of *P. aeruginosa* functions as a dynamic reservoir of resistance genes and virulence factors, serving as the core mechanism underlying persistent clinical infections (Silva et al., 2023). In the planktonic state, before biofilm formation, the bacteria rely on high metabolic activity and motility (e.g., flagellar-driven movement) to disseminate and initiate acute infections. This stage represents a

* Corresponding authao at: Mailing address: Shanghai Fengxian District Central Hospital, 6600 Nan Feng Rd., Shanghai 201499, China.
E-mail address: xiaolinlinshanghai@foxmail.com (L. Xiao).
[1] These authors contributed equally to this work.

https://doi.org/10.1016/j.crmicr.2025.100379

Available online 11 April 2025

therapeutic window due to high antibiotic permeability (sensitivity rate >90 %). However, once a biofilm forms, antibiotic susceptibility is reduced by 100 to 1000 times (Elmanama et al., 2020). For instance, ciprofloxacin's minimum inhibitory concentration (MIC) can increase from 0.5 μg/mL to 512 μg/mL, leading to treatment failure with conventional antibiotics (Akinduti et al., 2023). This surge in antibiotic resistance is driven by the orchestration of multiple hierarchical signaling networks: On one hand, the quorum sensing (QS) system (*Las/Rhl/Pqs*) orchestrates a cascade regulation of virulence factors, such as elastase *LasB* and alginate synthase *AlgD*, along with extracellular matrix components, including *Pel/Psl* polysaccharides and eDNA-rhamnolipid complexes (Liu et al., 2024). This coordination establishes a dual defense mechanism, comprising a physical barrier and an enhanced transmission system for resistance genes (Alcalde-Rico et al., 2020). On the other hand, the second messenger c-di-GMP, through a spatiotemporal gradient within the biofilm core (12 μM at the center vs. 1.2 μM at the periphery), induces persistent cell dormancy by reducing ATP synthesis (↓80 %), thereby reinforcing antibiotic tolerance (Abdelhafez et al., 2020). Simultaneously, the overexpression of the *MexAB-OprM* efflux pump further escalates bacterial resistance to a critical threshold (MIC >1024 μg/mL) (Laborda et al., 2023). Notably, in chronic lower limb infections, the ischemic microenvironment—characterized by hypoxia, iron restriction, and high shear stress—further enhances the biofilm formation capacity and antibiotic resistance of *P. aeruginosa* (Bhandari et al., 2022). Studies have shown that local hypoxia in diabetic foot ulcers (pO_2 <10 mmHg) activates c-di-GMP synthesis via the Anr-FNR system, leading to a surge in alginate concentration (12.7 mg/mL), which forms an osmoprotective barrier that severely restricts antibiotic penetration (<10 %) (Ugwuanyi et al., 2021). Meanwhile, the iron chelator pyoverdine hijacks host transferrin, increasing iron uptake efficiency sixfold, subsequently triggering MexCD-OprJ efflux pump-mediated polymyxin resistance (100-fold increase in resistance) (Kello et al., 2023). Clinical data indicate that the amputation risk in lower limb infections is 41 %, significantly higher than in other infection sites, and carbapenem treatment failure rates reach 38 % in biofilm-positive patients (Akinduti et al., 2023). However, current therapies (e.g., nano-catalytic clearance and QS inhibitors) remain limited by residual biofilm recurrence (28 %) and host toxicity concerns (mitochondrial ATP decrease to 40 %; Shakib et al., 2023). Therefore, a deeper investigation into the biofilm-forming capacity of *P. aeruginosa* is crucial for understanding its pathogenic mechanisms and developing innovative therapeutic strategies.

This study analyzed the biological characteristics of three *P. aeruginosa* strains isolated from a patient with a long-term lower limb infection. These strains exhibited distinct antimicrobial susceptibility profiles and biofilm-forming abilities, suggesting variations in virulence and resistance traits. Using a comprehensive set of experimental approaches, including antimicrobial susceptibility testing, multilocus sequence typing (MLST) (Williams et al., 2015), biofilm-associated gene profiling, growth curve analysis, Galleria mellonella infection assays, whole-genome sequencing, and bioinformatics analysis, we sought to uncover their genetic diversity, resistance, and virulence gene profiles, as well as their potential evolutionary trajectories within the host.

The findings of this study provide valuable insights into the behavior of *P. aeruginosa* during chronic infections and contribute to the development of new therapeutic strategies. By advancing our understanding, we aim to equip clinicians with more effective tools to combat this challenging pathogen.

2. Materials and methods

2.1. Isolation and identification of strains

Three *P. aeruginosa* strains were isolated in 2023 from pus samples of a patient with chronic bilateral lower limb infections at Fengxian Hospital, affiliated with Southern Medical University. Reference strains *P. aeruginosa* ATCC 27853 and *Escherichia coli* ATCC 25922 were obtained from the Shanghai Clinical Laboratory Quality Control Center. Strain identification was confirmed using the Bruker MALDI Biotyper™ and BioMerieux VITEK2 compact systems.

2.2. Antimicrobial susceptibility testing

The antimicrobial susceptibility of the three *P. aeruginosa* strains was evaluated using the Kirby–Bauer disk diffusion method and the broth microdilution method. Thirteen antibiotics were tested, including amikacin, aztreonam, ceftazidime, ciprofloxacin, colistin, cefepime, imipenem, levofloxacin, meropenem, cefoperazone, tigecycline, tobramycin, and piperacillin/tazobactam. The results were interpreted according to the guidelines of the Clinical and Laboratory Standards Institute (2023).

2.3. MLST typing

MLST typing of the three *P. aeruginosa* strains was conducted using primers targeting seven housekeeping genes (*adk, frdB, gyrB, icd, mdh, purA,* and *recA*), as per the Warwick MLST database (http://mlst.warwick.ac.uk/mlst/). Primer sequences and target fragment sizes were referenced from the literature (Bustin, 2000; Schmittgen and Zakrajsek, 2000; Vandesompele et al., 2002). DNA sequences were analyzed with DNAStar and matched to the MLST database (http://pubmlst.org/paeruginosa/) to determine sequence types (STs).

2.4. Detection of biofilm-related genes

A quantitative polymerase chain reaction (qPCR) was used to detect biofilm-related genes (*algD, pelA, pslA, rhlA, lasR*, and *lasI)* in the three *P. aeruginosa* strains (Franklin et al., 2011; Savli et al., 2003). The primers were synthesized by Sangon Biotech (Shanghai) Co., Ltd. Bacterial genomic DNA was extracted using the Ezup Column Bacteria Genomic DNA Purification Kit (Catalog No. B618255-0100, Sangon Biotech)(Table 1). The housekeeping gene *proC* was used as an internal reference (Savli et al., 2003), three replicate wells were set up for each PCR reaction, and negative control wells were set up with sterile deionized water instead of the template DNA. PCR amplification included TB Green dye, 3.2 μL of water, 0.4 μL of each primer, and 1 μL of the template in a 10 μL reaction (Table 2), and the PCR amplification conditions were 95 °C for 15 s, 60 °C for 60 s, and 95 °C for 30 s. Melting curve analysis was completed at 60 °C for 15 s (Table 3).

2.5. Growth curve analysis

The growth curves of five strains (the three isolated *P. aeruginosa* strains, *P. aeruginosa* ATCC 27853, and *E. coli* ATCC 25922) were measured using a Bioscreen C automated growth analyzer at 37 °C. Bacterial cultures were diluted in a liquid medium to 10^7–10^8 colony-forming units (CFU)/mL and inoculated into 100-well honeycomb plates with 200 μL per well. Wells containing only the medium served as negative controls. Plates were incubated at 37 °C for 24 h, with optical density (OD600) measurements taken every 30 min after shaking for 20 s three times for homogenization.

2.6. Biofilm formation assay

The bacterial suspension was diluted to 10^7 CFU/mL, and 100 μL of the bacterial solution was aspirated and added to a 96-well cell culture plate. Three replicate wells were made for each strain of bacteria. Three negative control wells were added with 100 μL of LB liquid medium per well and incubated at 37 ℃ for 72 h. The liquid medium was aspirated, and the wells were cleaned with an isotonic sodium chloride solution three times to remove the planktonic bacteria and then left to air dry at 37℃. Each well was fixed with methanol, stained with 0.1 % crystal violet 100 μL for 15 min, discarded the staining solution, and dried at 37

Table 1
Primer sequences for biofilm formation-related genes.

Gene	Forward primer(5′–3′)	Reverse primer(5′–3′)	Size(bp)
proC	CAGGCCGGGCAGTTGCTGTC	GGTCAGGCGCGAGGCTGTCT	180
pslA	GGCCTGTTTCCCTACCT	GCGGATGTCGTGGTTG	207
algD	CGAGAAGTCCGAACGCCACAC	ATCGGCGGGAAGTCGTA	186
pelA	GGCCTGCTCGAATACCTC	TGACCTTGAGTTTCTGCGACA	265
lasI	ACAAATTGGTCGGCGCGAAGAG	GCATGTAGGGGCCAGTGGTATC	230
lasR	GAAGATGGCGAGCGACCTTGGATTC	CTCGTGCTGCTTTCGCGTCTGGTAG	229
rhlA	CGCCTGAAAGCCAGCAACCATC	GTGCCCTCCACCCGCGAGAAAC	242

Table 2
PCR reaction system.

Component	Volume (μL)
TB Green qPCR Mix (2×)	5.0
Nuclease-free water	3.2
Forward primer	0.4
Reverse primer	0.4
Template DNA	1.0
Total volume	10

Table 3
PCR amplification conditions.

Step	Temperature (°C)	Time
Initial denaturation	95	15 s
Amplification cycles	95	15 s
	60	60 s
	95	30 s
Melting curve analysis	60	15 s

℃, and each well was rinsed slowly with 95 % ethanol for 3 times to remove the unbound dye and then dried at 37 ℃. Absorbance at 595 nm was measured using a zymograph, with the OD value of uninfected wells serving as the negative control (ODc). Biofilm formation was assessed based on ODc, where samples with absorbance ≤ ODc were classified as non-biofilm-forming; those > ODc but ≤ 2× ODc as weak biofilm formers; those > 2× ODc but ≤ 4× ODc as moderate biofilm formers; and those > 4× ODc as strong biofilm formers (Jerzsele et al., 2014).

2.7. Galleria mellonella infection assay

Six-week-old Galleria mellonella larvae (length ~2 cm, weight ~300 mg) were used for the infection assays. The larvae were maintained at 15 °C and acclimated at 37 °C for 4 h before infection. Bacterial suspensions of varying concentrations (1×10^3–1×10^6 CFU/mL) were prepared, and 10 μL was injected into the right proleg of each larva. After injection, the larvae were incubated at 37 °C in the dark, and their survival was monitored every 12 h to determine the time required to achieve 80 % mortality (LT_{80}) and the lethal dose causing 80 % mortality (LD_{80}). The larvae were considered to be dead if unresponsive or blackened. Data were analyzed using GraphPad Prism 6.0, with survival curves assessed via log-rank tests (SPSS and SAS software), and statistical significance was set at $p < 0.05$.

2.8. Whole-genome sequencing and bioinformatics analysis

Genomic DNA was extracted using the Ezup Column Bacteria Genomic DNA Purification Kit (Catalog No. B618255-0100, Sangon Biotech) and sequenced on the Illumina HiSeq 2500 platform by Novogene Co., Ltd. Assembly was performed using SPAdes software, with annotations provided by the RAST server. Whole-genome data were analyzed using ResFinder 4.4, LRE-Finder, VirulenceFinder 2.0, MLST 2.0, and PathogenFinder (https://cge.food.dtu.dk). And batch screening and detection of resistance genes and virulence genes in the genome from databases (e.g. CARD, VFDB) by ABRicate software. Phylogenetic trees were compared using MEGA X software and ClustalW and constructed by the neighbor-joining method with 1000 bootstrap repetitions using KSNP v4.1 software.

3. Results

3.1. Antimicrobial susceptibility testing

Antimicrobial susceptibility testing was performed on the three *P. aeruginosa* strains isolated from a patient with lower limb ulcers related to a vascular condition. The results revealed significant differences in antibiotic sensitivity among the strains. The strain WYDPA-23-1 was sensitive to amikacin, ceftazidime, ciprofloxacin, colistin, cefepime, imipenem, meropenem, levofloxacin, tobramycin, and piperacillin/tazobactam but resistant to tigecycline. The strain WYDPA-23-2 was sensitive to amikacin, ceftazidime, colistin, imipenem, and meropenem but resistant to aztreonam, ciprofloxacin, levofloxacin, cefoperazone/sulbactam, piperacillin/tazobactam, tigecycline, and gentamicin. In contrast, the strain WYDPA-23-3 exhibited multidrug resistance, showing no sensitivity to any of the tested antibiotics (Table 4).

3.2. Biofilm formation ability

The results demonstrated that all three *P. aeruginosa* strains harbored key biofilm-related genes, including *algD, pelA, pslA, rhlA, lasR, and lasI*. Compared with the other strains, WYDPA-23-3 exhibited significantly higher expression levels of *algD, pslA, lasR,* and *lasI* ($p < 0.0001$). Additionally, the expression of *pelA* and *pslA* varied significantly among different strains ($p < 0.05$ to $p < 0.01$). However, no significant difference was observed in *rhlA* expression across the strains ($p > 0.05$). Specifically, *pelA* expression was significantly higher in the WYDPA-23-

Table 4
Drug susceptibility testing results of different *P. aeruginosa* strains.

Antibiotic type	WYDPA–23-1	WYDPA–23-2	WYDPA–23-3	Method
AMK	S (8)	S (≤2)	S (16)	MIC
ATM	S (4)	R (≥64)	R (32)	MIC
CAZ	S (2)	S (2)	R (≥64)	MIC
CIP	S (≤0.25)	I (1)	R (≥4)	MIC
COL	S (2)	S (2)	S (2)	MIC
FEP	S (8)	S (8)	R (≥32)	MIC
IMP	S (2)	S (2)	R (≥16)	MIC
LVX	S (1)	R (4)	R (≥8)	MIC
MEM	S (1)	S (1)	R (≥16)	MIC
CFP/SU	S (≤8)	I (32)	R (≥64)	MIC
TGC	R (≥8)	R (≥8)	R (≥8)	MIC
TOB	S (≤1)	S (≤1)	R (≥16)	MIC
TZP	S (≤4)	I (32)	R (≥128)	MIC
GEN	S (18)	S (18)	R (6)	MIC
PIP	–	I (21)	R (13)	MIC

MIC, minimum inhibitory concentration; s, sensitive; I, intermediate; r, resistant; ND, no data were provided in the corresponding document; AMK, amikacin; ATM, aztreonam; CAZ, ceftazidime; CIP, ciprofloxacin; COL, colistin; FEP, cefepime; IMP, imipenem; LVX, levofloxacin; MEM, meropenem; CFP, cefoperazone; TGC, tigecycline; TOB, tobramycin; TZP, piperacillin/tazobactam; GEN, gentamicin; PIP, piperacillin.

2 strain than in WYDPA-23-1 and WYDPA-23-3, whereas *pslA* expression was markedly lower in WYDPA-23-2 compared to the other two strains.

Biofilm formation ability was also assessed using crystal violet staining, which showed statistically significant differences among the strains. Among them, WYDPA-23-2 showed the strongest biofilm formation ability with thicker and denser biofilm structures. Significant differences in biofilm formation were also observed between WYDPA-23-2 and WYDPA-23-3, which further highlighted the phenotypic differences between the strains (Figs. 1 and 2).

3.3. Carriage of resistance and virulence genes

MLST typing revealed that strain WYDPA-23-1 belonged to ST381, WYDPA-23-2 to ST270, and WYDPA-23-3 to ST2584. Analysis of sequencing data showed the presence of virulence genes such as *algB, plcH, phzH, lasB, exoT, pilB, pilS, pilR, pvdA, pvdQ, pvdL, pvdH, pvdG,* and *pvdS* in all three strains, though the percentage of similarity in these genes varied among the strains (Fig. 3). Certain virulence genes, including *vgrG1b, hcp1, pilA,* and *exoY,* were present in some strains but absent in others, highlighting significant differences in the virulence gene profiles of the three strains.

Regarding resistance genes, the three strains showed high similarity, particularly in the carriage of key genes associated with multidrug efflux pump systems. All strains carried multiple resistance genes, including *blaOXA-50, fosA, catB7, sul1, aph(3′)-IIb, bcr-1*, and genes related to efflux pump systems. These genes conferred resistance to a wide range of antibiotics, including multiple drug classes, cephalosporins, penicillins, triclosan, aminoglycosides, sulfonamides, phenols, β-lactams, and bicyclomycin. Notably, the *aac(6′)-Ib9* gene, associated with aminoglycoside resistance, was detected in WYDPA-23-2 but was absent in WYDPA-23-1 and WYDPA-23-3. The *dfrA27* gene, related to dihydrofolate reductase and potentially influencing susceptibility to certain antibiotics, was found in WYDPA-23-1 and WYDPA-23-2 but was absent in WYDPA-23-3.

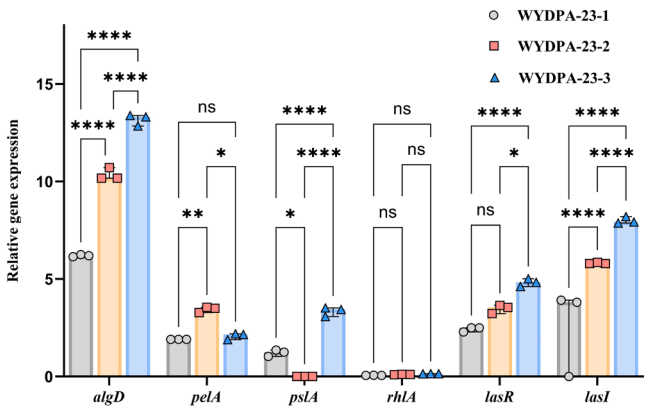

Fig. 2. Abundance plot of biofilm formation genes for three *P. aeruginosa* strains. Data are presented as median with interquartile range. Statistical significance was determined using two-way ANOVA followed by multiple comparison tests. Asterisks denote significant differences among the same type of genes across different strains: $p < 0.05$: *; $p < 0.01$: **; $p < 0.001$: ***; $p < 0.0001$: ****; $p \geq 0.05$: ns (not significant). All gene expression data were normalized to the *proC* reference gene and adjusted based on the DNA concentration of each sample.

3.4. Growth curve analysis

Growth curves derived from Bioscreen C measurements over 24 h (Fig. 4) revealed differences in growth trends among the five strains (WYDPA-23-1, WYDPA-23-2, WYDPA-23-3, ATCC 27853, and ATCC 25922) at 37 °C. The strains WYDPA-23-1 and WYDPA-23-2 displayed similar growth patterns, whereas WYDPA-23-3 exhibited the fastest growth rate and WYDPA-23-2 the slowest. Overall, the growth trends of the *P. aeruginosa* strains surpassed those of the standard *E. coli* strain ATCC 25922. As the bacterial growth curves generally follow an S-shaped pattern, this study focused on strains during the exponential growth phase for analysis, with the observed curves primarily representing the logarithmic growth phases.

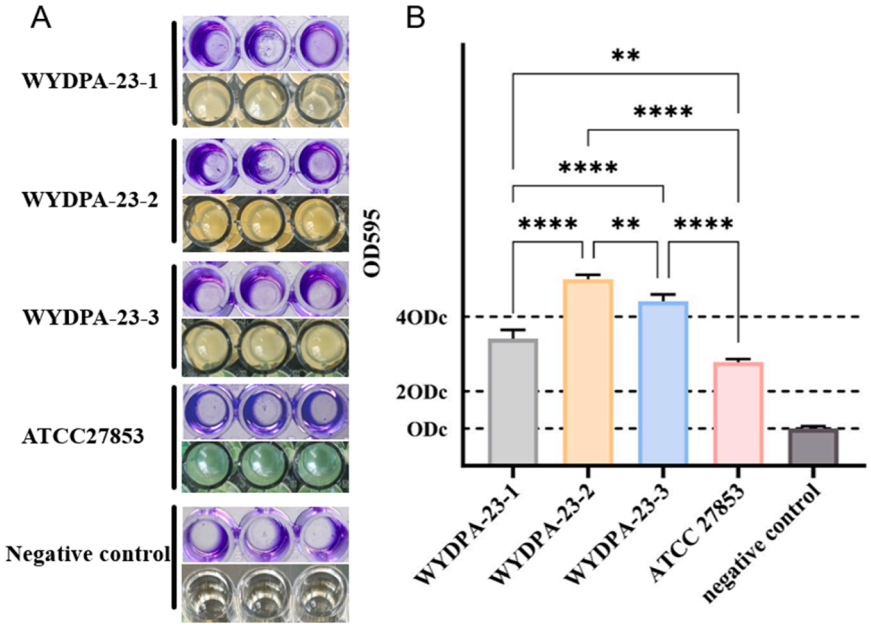

Fig. 1. Biofilm formation of *P. aeruginosa* strains after 72 h of cultivation. (A) Standard *P. aeruginosa* ATCC 27853 was used as the positive control group, and *E. coli* ATCC 2522 was used as the negative control group. Biofilm formation after staining with crystal violet and turbidity of the medium 24 h before unstaining are shown. (B) Data are expressed as mean ± standard deviation. Statistical significance was analyzed by one-way analysis of variance (ANOVA) followed by appropriate post hoc tests. Asterisks indicate significant differences in biofilm formation ability between strains: $p < 0.05$: *; $p < 0.01$: **; $p < 0.001$: ***; $p < 0.0001$: ****; $p \geq 0.05$: ns (not significant).

Gene	WYDPA-23-1	WYDPA-23-2	WYDPA-23-3	Gene	WYDPA-23-1	WYDPA-23-2	WYDPA-23-3	Gene	WYDPA-23-1	WYDPA-23-2	WYDPA-23-3
exoY	+	+	+	*AAC(3)-IId*	-	+	-	*mexA*	+	+	+
hcp1	+	+	+	*AAC(6')-Ib9*	-	+	-	*mexB*	+	+	+
lasB	+	+	+	*APH(3'')-Ib*	-	+	-	*mexE*	+	+	+
exoT	+	+	+	*APH(6)-Id*	-	+	-	*mexF*	+	+	+
pilB	+	+	+	*bcr-1*	+	+	+	*mexJ*	+	+	+
pilS	+	+	+	*catB7*	+	+	+	*mexK*	+	+	+
pilR	+	+	+	*dfrA27*	+	-	-	*mexL*	+	+	+
pvdA	+	+	+	*emrE*	+	+	+	*mexM*	+	+	+
pvdQ	+	+	+	*fosA*	+	+	+	*mexN*	+	+	+
pvdL	+	+	+	*OXA-486*	-	+	-	*muxA*	+	+	+
pvdH	+	+	+	*OXA-50*	+	+	+	*muxB*	+	+	+
pvdG	+	+	+	*PDC-3*	+	-	+	*muxC*	+	+	+
pvdS	+	+	+	*PDC-8*	-	+	-	*opmB*	+	+	+
algB	+	+	-	*soxR*	-	-	+	*opmE*	+	+	+
plcH	+	+	-	*sul1*	+	+	-	*opmH*	+	+	+
vgrG1b	-	+	+	*triA*	+	+	+	*oprM*	+	+	+
phzH	+	+	-	*triB*	+	+	+	*oprN*	+	+	+
pilA	-	-	+	*triC*	+	+	+	*pmpM*	+	+	+

Fig. 3. Carriage of virulence genes and drug resistance genes of three *P. aeruginosa* strains (WYDPA-23-1, WYDPA-23-2, and WYDPA-23-3). This table illustrates the presence (+) or absence (-) of various genes related to biofilm formation and antimicrobial resistance across the three *P. aeruginosa* strains. The listed genes include those involved in biofilm formation (e.g., *exoY, hcp1, lasB*) and antimicrobial resistance (e.g., *AAC(3)-IId, macA, opmB*). Each row represents a specific gene, and the columns correspond to the three bacterial strains.

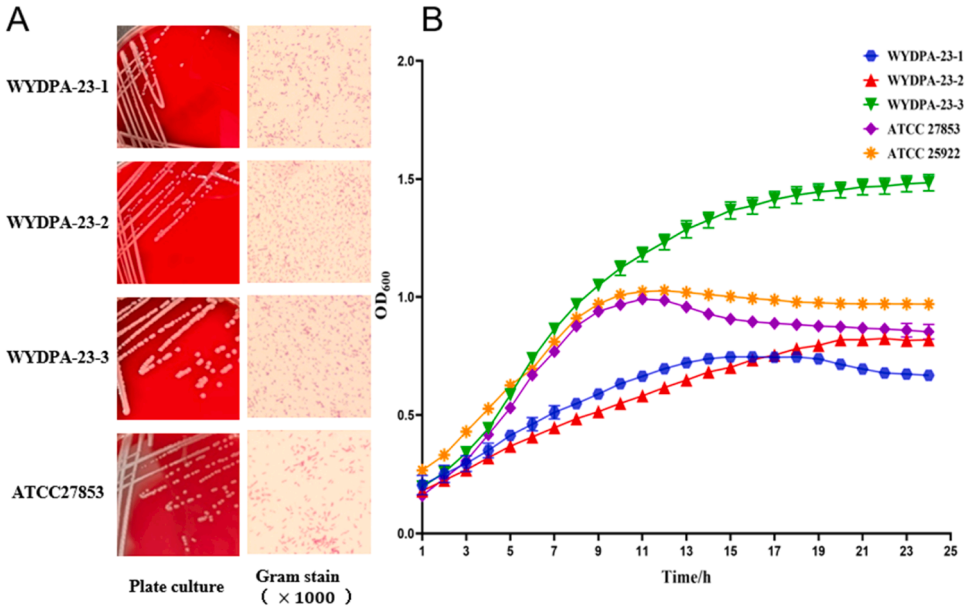

Fig. 4. Growth curves of different strains over 24 h(37℃). (A) Colony morphology of different strains of each strain and the corresponding Gram-stained microscopic morphology of each strain after 24 h of incubation in blood plates at a magnification of ×1000. (B) Variation of each strain in the growth curve. The results show that WYDPA-23-1 (green) grew the fastest, followed by WYDPA-23-2 (blue), WYDPA-23-3 (red), and the reference strains (ATCC 27853, purple, and ATCC 25922, orange). Data points indicate the mean of three biological replicates, and error bars indicate standard deviation. (For interpretation of the references to color in this figure legend, the reader is referred to the web version of this article.).

3.5. *Galleria mellonella survival assay*

For each of the three isolated strains and the ATCC 27,853 reference strain, bacterial suspensions with four concentrations ranging from 1×10^3 to 1×10^6 CFU/mL were prepared and injected into Galleria mellonella larvae. The number of larval deaths was recorded at 12, 24, 36, 48, and 72 h post-injection. The LT_{80} and LD_{80} at the same concentration were calculated from the average of three independent experiments (Table 5).

The results showed that the LT_{80} value for the strain WYDPA-23-3 was significantly higher than that for the other strains, with some larvae remaining alive at 72 h. The survival curves (Fig. 5) indicated that larval lethality was strain-dependent and exhibited a dose-dependent

Table 5
Experimental group LT_{80} for different strains of bacteria.

Concentration(CFU/mL)	LT_{80} (h)			
	WYDPA-23-1	WYDPA-23-2	WYDPA23-3	ATCC27853
10^6	12	12	24	12
10^5	12	12	28	36
10^4	16	24	52	12
10^3	40	24	28	32

LT_{80}: represents the time required to cause 80 % mortality of the host at each concentration. CFU: colony-forming units.

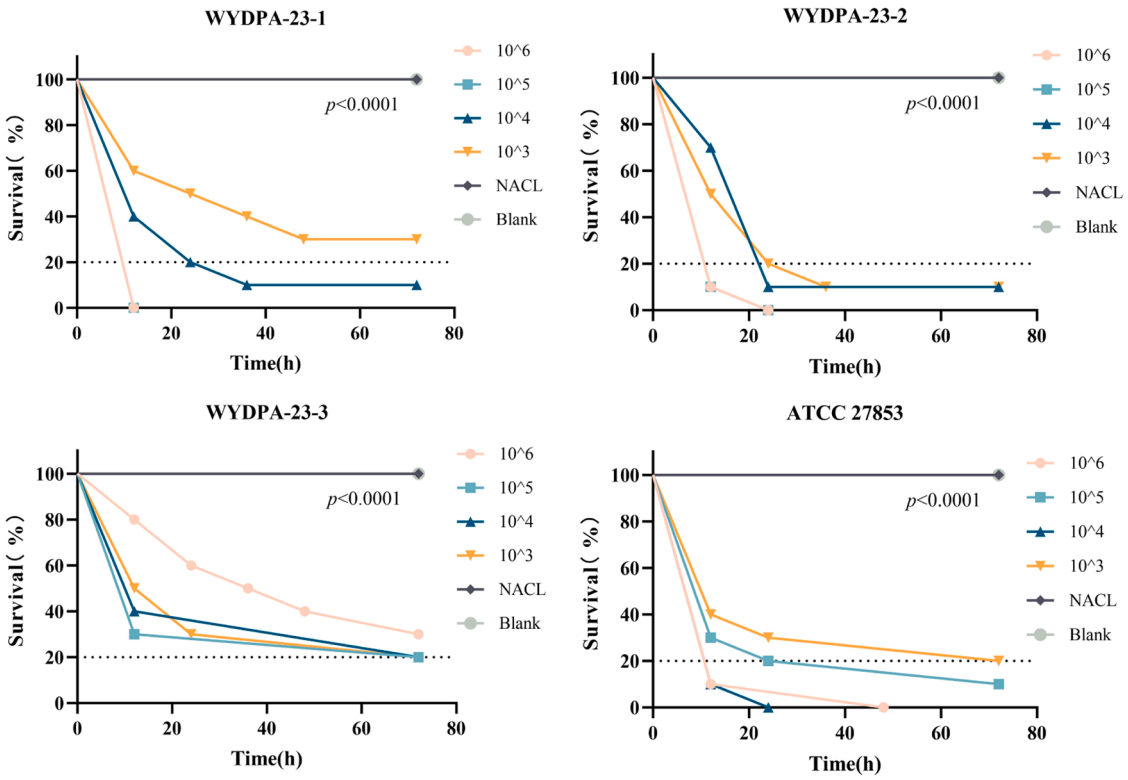

Fig. 5. Survival curves of Galleria mellonella infection with *P. aeruginosa*. The graph shows the survival rate of three *P. aeruginosa* strains (WYDPA-23-1, WYDPA-23-2, WYDPA-23-3) and the reference strain ATCC 27853 at different bacterial concentrations (1×10^6, 10^5, 10^4, 10^3 CFU/mL) over 3 days. Survival is plotted as a percentage of time (hours). The dashed line represents baseline survival. Data points are shown as mean values, and error bars indicate standard deviation. Statistical significance between groups is indicated by $p < 0.0001$. The results showed a significant dose-dependent decrease in survival rate with increasing bacterial concentration.

trend, with LT_{80} values decreasing as the bacterial concentration increased. Notably, larvae injected with WYDPA-23-1, WYDPA-23-2, and the ATCC 27853 reference strain had significantly lower LT80 values than larvae injected with WYDPA-23-3. In the concentration range of 10^6–10^5 CFU/mL, the LD_{80} values for WYDPA-23-1, WYDPA-23-2, and ATCC 27853 were significantly higher than those for WYDPA-23-3 at 12 h post-injection. Specifically, the LD_{80} concentrations for WYDPA-23-1, WYDPA-23-2, and ATCC 27853 were 1×10^6 CFU/mL at

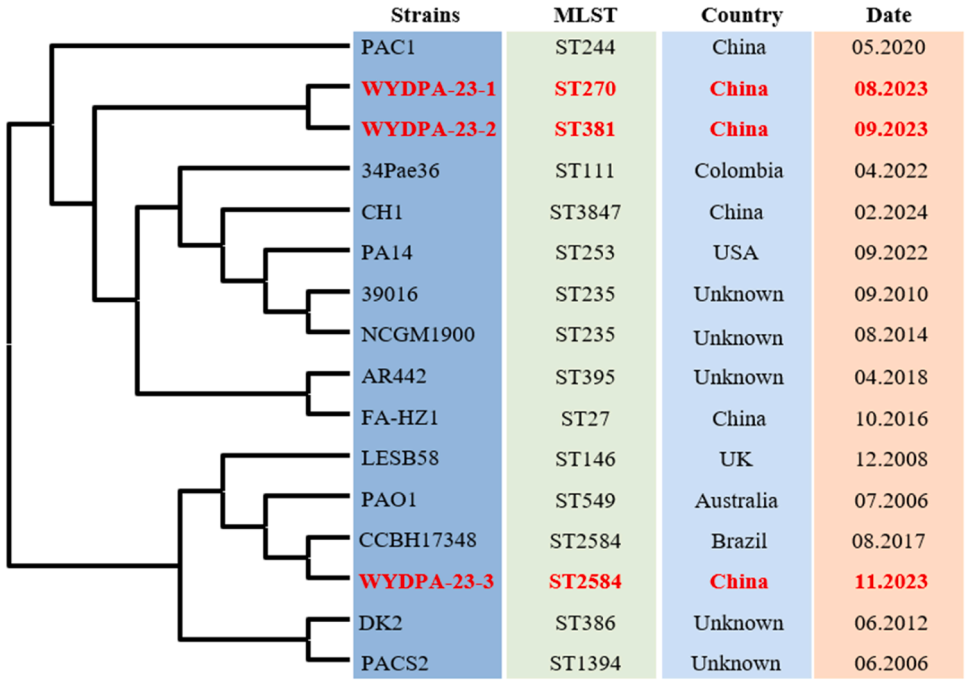

Fig. 6. Evolutionary analysis of the phylogenetic tree. Red indicates the strains discussed in the present study. MLST, multilocus sequence typing.

12 h, whereas WYDPA-23-3 did not reach 80 % mortality at the same time point.

3.6. Phylogenetic analysis

This study included a detailed phylogenetic analysis of the three *P. aeruginosa* strains (WYDPA-23-1, WYDPA-23-2, WYDPA-23-3) isolated from the same patient at different times between August and November 2023 in China. MLST typing identified the strains as ST381, ST270, and ST2584, revealing genetic diversity within the same host. The different sequence types of WYDPA-23-1 and WYDPA-23-2 suggest notable genetic differences and potentially distinct evolutionary pathways within the host.

Interestingly, the strain WYDPA-23-3 shared the ST2584 type with the strain CCBH17348, previously isolated in Brazil. This finding highlights both the genetic diversity among strains within a single patient and the possibility of global dissemination events or a shared ancestral origin (Fig. 6). The observed genetic diversity in a single host may be linked to the strain's adaptability, development of resistance, or other biological characteristics. The ST2584 shared type between WYDPA-23-3 and CCBH17348, despite their geographical separation, suggests potential global transmission patterns or horizontal gene transfer among strains.

4. Discussion

P. aeruginosa is a major pathogen in chronic infections, particularly in immunocompromised individuals and patients with underlying vascular diseases (Elmanama et al., 2020). Its antibiotic resistance and biofilm-forming capacity make treatment highly challenging (Ciofu and Tolker-Nielsen, 2019). The findings of this study indicate significant differences in antibiotic susceptibility among three *P. aeruginosa* strains isolated from the wound of a patient with lower limb arteriosclerosis obliterans and chronic ulcers. Specifically, WYDPA-23-1 was susceptible to multiple antibiotics, WYDPA-23-2 exhibited moderate resistance, whereas WYDPA-23-3 displayed multidrug resistance (MDR), being resistant to all tested antibiotics. This finding aligns with previous studies suggesting that *P. aeruginosa* can exhibit highly heterogeneous resistance profiles even within the same host (Wahyudi et al., 2019).

Furthermore, in patients with chronic lower limb infections, inadequate tissue perfusion and persistent inflammation create a hypoxic and ischemic microenvironment that promotes accelerated biofilm formation, enhanced virulence, and adaptive antibiotic resistance evolution (Reza and Behnaz, 2013). Biofilms serve as a "reservoir" of critical virulence factors in *P. aeruginosa*, enabling the bacteria to effectively and persistently evade host immune defenses and antibiotic treatment (Al-Wrafy et al., 2017). This study found that all three strains harbored key biofilm-associated genes, including *algD, pelA, pslA, rhlA, lasR,* and *lasI,* though their expression levels varied significantly. Notably, while WYDPA-23-2 exhibited the highest expression levels of *algD, pslA, lasR,* and *lasI,* it also showed significantly higher *pelA* expression than the other two strains and demonstrated the strongest biofilm formation capacity, a finding further confirmed by crystal violet staining. Previous studies have shown that the *pelA* gene plays a crucial role in extracellular polysaccharide synthesis, contributing to biofilm stability (Farhan et al., 2023). Although WYDPA-23-2 exhibited lower *pslA* expression, it still formed the strongest biofilm, suggesting that biofilm architecture is influenced by multiple regulatory mechanisms, including alternative polysaccharide synthesis pathways or quorum sensing systems (Al-Enazi, 2024). These findings highlight the genetic and phenotypic diversity of *P. aeruginosa* within the same host, further emphasizing the complexity of biofilm formation in chronic infections (Hassan et al., 2020).

The MLST typing results further revealed significant genetic diversity of *P. aeruginosa* within the same host, with WYDPA-23-1, WYDPA-23-2, and WYDPA-23-3 classified as ST381, ST270, and ST2584, respectively. Virulence gene analysis revealed the presence of several genes, including *algB, plcH, phzH, lasB, exoT, pilB, pilS, pilR, pvdA, pvdQ, pvdL, pvdH, pvdG,* and *pvdS*, in all three strains, albeit with varying percentages of similarity. However, certain virulence genes (*vgrG1b, hcp1, pilA,* and *exoY*) were present in some strains and absent in others, indicating substantial differences in the strains' virulence gene profiles. The three strains exhibited high similarity in resistance gene carriage, especially for genes related to multidrug efflux pump systems (Horna and Ruiz, 2021; Sawa et al., 2014). All three strains carried multiple resistance genes, such as *blaOXA-50, fosA, catB7, sul1, aph(3′)-IIb,* and *bcr-1*, conferring resistance to various antibiotic classes, including cephalosporins, penicillins, aminoglycosides, and β-lactams (Ahmed, 2022; Ito et al., 2017; Venkatesan et al., 2023). Notably, the *aac(6′)-Ib9* gene, which is associated with aminoglycoside resistance, was detected in WYDPA-23-2 only, whereas the *dfrA27* gene, which is linked to dihydrofolate reductase activity, was absent in WYDPA-23-3 but present in WYDPA-23-1 and WYDPA-23-2.

Growth curve analysis demonstrated that all three *P. aeruginosa* strains grew faster than the standard *E. coli* strain ATCC 25922, probably because of their higher metabolic activity and adaptability. The strain WYDPA-23-3 exhibited the fastest growth rate, which may correlate with its strong biofilm-forming ability and multidrug resistance. These characteristics likely enhanced WYDPA-23-3′s competitive advantage within the host, impacting the infection's treatment and prognosis.

The Galleria mellonella infection assays demonstrated strain-dependent lethality, with a dose-dependent relationship between bacterial concentration and mortality. Notably, the strain WYDPA-23-3 had significantly higher LT80 values than the other strains, suggesting that its strong biofilm-forming ability and multidrug resistance (Kulayta et al., 2024) might delay its lethality. These results highlight the need for more aggressive treatment strategies, such as higher antibiotic doses or combination therapies, against strains with strong biofilm-forming capabilities and multidrug resistance.

Phylogenetic analysis revealed that the three *P. aeruginosa* strains, which had been isolated from the same patient within a few months of each other, displayed different ST types, indicating extensive genetic diversity within a single host (Weimann et al., 2024). Strain WYDPA-23-3 shared the ST2584 type with strain CCBH17348, previously isolated in Brazil, suggesting potential global dissemination events or a shared ancestral origin. This genetic diversity within a single host may be associated with the strains' adaptability, resistance development, or other biological changes (Clark et al., 2018; Ekroth et al., 2021). The similarity between strains WYDPA-23-3 and CCBH17348, despite geographic separation, points to potential global transmission patterns or horizontal gene transfer among strains. This finding is consistent with previous epidemiological studies of clinical strains, indicating that the genetic adaptability of *P. aeruginosa* plays a crucial role in its persistent infections and the evolution of antibiotic resistance.

In summary, this study revealed significant differences in the biofilm-forming ability, resistance profiles, and virulence gene carriage among different ST types of *P. aeruginosa*, as well as the potential impact of these differences on the treatment of the infection. These findings provide important clinical insights, particularly for selecting antibiotics and developing treatment strategies. Future research should explore the mechanisms driving genetic variation among these strains and their implications for infections' progression and treatment outcomes. Additionally, further studies are needed to develop novel therapies targeting strains with strong biofilm-forming capabilities and multidrug resistance.

5. Conclusion

In this study, we report a unique 30-year chronic infection from which three distinct *P. aeruginosa* subtypes were isolated. The findings revealed a novel microbial coexistence model where different subtypes of the same bacterial species coexisted within the host, collectively

influencing disease progression—an aspect not readily detected by current diagnostic methods. Among the strains, the ST270 subtype exhibited the strongest biofilm-forming capacity and highest virulence, potentially linked to its downregulated *pelA* gene expression, in line with previous research. Moreover, the capacity for biofilm formation was positively correlated with treatment duration, indicating that more robust biofilms require longer interventions (Qin et al., 2022). Phylogenetic analysis also uncovered marked genetic diversity, suggesting possible global dissemination or a shared ancestral origin. These findings offer new insights into the role of *P. aeruginosa* in lower limb infections associated with vascular disease and underscore the importance of biofilm in therapeutic strategies. Future research should focus on developing precise methods to assess biofilm-forming capacity and creating novel therapeutic approaches targeting biofilm-forming and multidrug-resistant strains. However, given the limited sample size and focus on a single host, further studies with larger cohorts and multiple hosts are needed to clarify the genetic mechanisms underlying strain variation and their effects on infection progression and treatment outcomes.

Ethics statement

This study adhered to the principles of the Declaration of Helsinki, revised in 2013, and was approved by the Medical Ethics Committee of Fengxian District Central Hospital in Shanghai (Affiliated Sixth People's Hospital South Campus, Shanghai Jiaotong University; approval number SL2024-KY-22-01). These studies were conducted by local legislation and institutional requirements. The participants provided written informed consent to participate in this study. Personal written informed consent was obtained for any potentially identifiable images or data included in the publication of this article.

Declaration of competing interest

The authors declare that they have no known competing financial interests or personal relationships that could have appeared to influence the work reported in this paper.

Funding

This study was supported by grants from the National Key R&D Program Intergovernmental Key Special Projects (Grant No. 2024YFE0102600), the National Natural Science Foundation of China (Grant No. 82202589), Shanghai Sixth People's Hospital Medical Group, the Natural Science Project of Shanghai Health Medical College (Grant No.SSF-24-15-01), and Shanghai Municipal Health System Key Discipline Construction Project (Grant No.2024ZDXK0063).

Acknowledgments

We thank the South Hospital of the Sixth People's Hospital affiliated to Shanghai Jiaotong University for providing the laboratory and policy support for this study.

Supplementary materials

Supplementary material associated with this article can be found, in the online version, at doi:10.1016/j.crmicr.2025.100379.

Data availability

Data will be made available on request.

References

Abdelhafez, M.M., El-Ageery, S., Mohamed, S., Abd El-Aal, S., 2020. Efflux pump inhibition versus quorum sensing inhibition in hospital-acquired multidrug-resistant Pseudomonas aeruginosa isolates in Mansoura University Hospitals. Egypt. J. Med. Microbiol. 29, 1–9. https://doi.org/10.21608/ejmm.2020.28752.

Ahmed, O.B., 2022. Detection of antibiotic resistance genes in *Pseudomonas aeruginosa* by whole genome sequencing. Infect. Drug Resist. 15, 6703–6709. https://doi.org/10.2147/IDR.S389959.

Akinduti, P., George, O.W., Ohore, H.U., Ariyo, O.E., Popoola, S.T., Adeleye, A., Akinwande, K., Popoola, J., Rotimi, S., Olufemi, F.O., Omonhinmin, C., Olasehinde, G., 2023a. Evaluation of efflux-mediated resistance and biofilm formation in virulent Pseudomonas aeruginosa associated with healthcare infections. Antibiotics 12, 1248. https://doi.org/10.3390/antibiotics12081248.

Alcalde-Rico, M., Olivares-Pacheco, J., Halliday, N., Cámara, M., Martínez, J.L., 2020. The analysis of the role of MexAB-OprM on quorum sensing homeostasis shows that the apparent redundancy of Pseudomonas aeruginosa multidrug efflux pumps allows keeping the robustness and the plasticity of this intercellular signaling network. bioRxiv. https://doi.org/10.1101/2020.03.10.986737.

Al-Enazi, N.M., 2024. Evaluation of biofilm formation and expression of *psl, pel, alg* genes of Pseudomonas aeruginosa in exposure to detergents. Acta Microbiol. Immunol. Hung 71 (2), 127–133. https://doi.org/10.1556/030.2024.02277.

Al-Wrafy, F., Brzozowska, E., Górska, S., Gamian, A., 2017. Pathogenic factors of Pseudomonas aeruginosa—the role of biofilm in pathogenicity and as a target for phage therapy. Adv. Hyg. Exp. Med. 71, 78–91. https://doi.org/10.5604/01.3001.0010.3791.

Bhandari, S., Adhikari, S., Karki, D., Chand, A.B., Sapkota, S., Dhungel, B., Banjara, M., Joshi, P., Lekhak, B., Rijal, K., 2022. Antibiotic resistance, biofilm formation, and detection of mexA/mexB efflux-pump genes among clinical isolates of Pseudomonas aeruginosa in a tertiary care hospital, Nepal. Front. Trop. Dis. 3, 810863. https://doi.org/10.3389/fitd.2021.810863.

Bogiel, T., Depka, D., Kruszewski, S., 2023. Comparison of virulence-factor-encoding genes and genotype distribution amongst clinical Pseudomonas aeruginosa strains. Int. J. Mol. Sci. 24 (3), 2345. https://doi.org/10.3390/ijms24032345.

Boustanshenas, M., Bakhshi, B., Mobasseri, P., Kiani, P., Hajiyan Hossein Abadi, F., Seyfi, E., Majidpour, A., Mousavi Shabestari, T., 2023. Genetically diverse, extremely resistant, and pan-drug resistant Pseudomonas aeruginosa as the main cause of nosocomial infection among hospitalized patients. Arch. Clin. Infect. Dis. 18 (2), e136338. https://doi.org/10.5812/archcid-136338.

Brzozowski, M., Krukowska, Ż., Galant, K., Jursa-Kulesza, J., Kosik-Bogacka, D., 2020. Genotypic characterisation and antimicrobial resistance of Pseudomonas aeruginosa strains isolated from patients of different hospitals and medical centres in Poland. BMC Infect. Dis. 20, 693. https://doi.org/10.1186/s12879-020-05404-w.

Bustin, S., 2000. Absolute quantification of mRNA using real-time reverse transcription polymerase chain reaction assays. J. Mol. Endocrinol. 25 (2), 169–193. https://doi.org/10.1677/jme.0.0250169.

Ciofu, O., Tolker-Nielsen, T., 2019. Tolerance and resistance of Pseudomonas aeruginosa biofilms to antimicrobial agents—How P. aeruginosa can escape antibiotics. Front. Microbiol. 10, 913. https://doi.org/10.3389/fmicb.2019.00913.

Clark, S.T., Guttman, D.S., Hwang, D.M., 2018. Diversification of *Pseudomonas aeruginosa* within the cystic fibrosis lung and its effects on antibiotic resistance. FEMS Microbiol. Lett. (6), 365. https://doi.org/10.1093/femsle/fny026.

Ekroth, A.K.E., Gerth, M., Stevens, E.J., Ford, S.A., King, K.C., 2021. Host genotype and genetic diversity shape the evolution of a novel bacterial infection. ISME J. 15 (7), 2146–2157. https://doi.org/10.1038/s41396-021-00911-3.

Elmanama, A., Al-Sheboul, S., Abu-Dan, R.I., 2020a. Antimicrobial resistance and biofilm formation of Pseudomonas aeruginosa. Int. Arab. J. Antimicrob. Agents 10, 1–7. https://doi.org/10.3823/840.

Farhan, R.E., Solyman, S.M., Hanora, A.M., Azab, M.M., 2023. Molecular detection of different virulence factors genes harboring *pslA, pelA, exoS, toxA,* and *algD* among biofilm-forming clinical isolates of Pseudomonas aeruginosa. Cell. Mol. Biol. 69 (5), 32–39. https://doi.org/10.14715/cmb/2023.69.5.5.

Franklin, M.J., Nivens, D.E., Weadge, J.T., Howell, P.L., 2011. Biosynthesis of the *Pseudomonas aeruginosa* extracellular polysaccharides, alginate, Pel, and psl. Front. Microbiol. 2. https://doi.org/10.3389/fmicb.2011.00167.

Hassan, M.A.R., Musleh, L.N., Al-Mathkhury, H.F., 2020. Gene expression of *pelA* and *pslA* in Pseudomonas aeruginosa under gentamicin stress. Iraqi J. Sci. 61 (2), 295–305. https://doi.org/10.24996/ijs.2020.61.2.6.

Horna, G., Ruiz, J., 2021. Type 3 secretion system of *Pseudomonas aeruginosa*. Microbiol. Res. 246, 126719. https://doi.org/10.1016/j.micres.2021.126719.

Ito, R., Mustapha, M.M., Tomich, A.D., Callaghan, J.D., McElheny, C.L., Mettus, R.T., Shanks, R.M.Q., Sluis-Cremer, N., Doi, Y., 2017. Widespread fosfomycin resistance in gram-negative bacteria attributable to the chromosomal *fosA* gene. MBio 8 (4). https://doi.org/10.1128/mBio.00749-17.

Jerzsele, Á., Gyetvai, B., Csere, I., Gálfi, P., 2014. Biofilm formation in *Malassezia pachydermatis* strains isolated from dogs decreases susceptibility to ketoconazole and itraconazole. Acta Vet. Hung. 62 (4), 473–480. https://doi.org/10.1556/AVet.2014.019.

Kello, E., Greenberg, R., Li, W., Polansky, S., Maldonado, R., Peter, Y., Basu, P., 2023. The effect of antibiotic treatment and gene expression of MexB efflux transporters on the resistance in Pseudomonas aeruginosa biofilms. Appl. Microbiol. 3, 456–467. https://doi.org/10.3390/applmicrobiol3030034.

Kulayta, K., Zerdo, Z., Seid, M., Dubale, A., Manilal, A., Kebede, T., Alahmadi, R.M., Raman, G., Akbar, I., 2024. Biofilm formation and antibiogram profile of bacteria from infected wounds in a general hospital in southern Ethiopia. Sci. Rep. 14 (1), 26359. https://doi.org/10.1038/s41598-024-78283-9.

Laborda, P., Lolle, S., Hernando-Amado, S., Alcalde-Rico, M., Martínez, J.L., Molin, S., Johansen, H.K., 2023. Efflux pump mutations in Pseudomonas aeruginosa cause low-level clinical resistance and high-level tolerance to antibiotics in patients. bioRxiv. https://doi.org/10.1101/2023.05.12.540546.

Liu, J., Liu, J., Huang, Y.-S., Chen, W.-M., Lin, J., 2024. Cyclic diguanylate G-quadruplex inducer-quorum sensing inhibitor hybrids as bifunctional anti-biofilm and anti-virulence agents against Pseudomonas aeruginosa. J. Med. Chem. 67, 5678–5690. https://doi.org/10.1021/acs.jmedchem.4c01253.

Pusic, P., Sonnleitner, E., Bläsi, U., 2021. Specific and global RNA regulators in Pseudomonas aeruginosa. Int. J. Mol. Sci. 22 (12), 6372. https://doi.org/10.3390/ijms22126372.

Qin, S., Xiao, W., Zhou, C., Pu, Q., Deng, X., Lan, L., Liang, H., Song, X., Wu, M., 2022. *Pseudomonas aeruginosa*: pathogenesis, virulence factors, antibiotic resistance, interaction with host, technology advances and emerging therapeutics. Signal Transd. Target. Ther. 7 (1), 199. https://doi.org/10.1038/s41392-022-01056-1.

Reza, G., Behnaz, S.E., 2013. Effects of oxygen on in-vitro biofilm formation and antimicrobial resistance of Pseudomonas aeruginosa. Pharm. Sci. 19 (2), 96–99. https://doi.org/10.5681/PS.2013.096.

Savli, H., Karadenizli, A., Kolayli, F., Gundes, S., Ozbek, U., Vahaboglu, H., 2003. Expression stability of six housekeeping genes: a proposal for resistance gene quantification studies of *Pseudomonas aeruginosa* by real-time quantitative RT-PCR. J. Med. Microbiol. 52 (5), 403–408. https://doi.org/10.1099/jmm.0.05132-0.

Sawa, T., Shimizu, M., Moriyama, K., Wiener-Kronish, J.P., 2014. Association between *Pseudomonas aeruginosa* type III secretion, antibiotic resistance, and clinical outcome: a review. Crit. Care 18 (6), 668. https://doi.org/10.1186/s13054-014-0668-9.

Schmittgen, T.D., Zakrajsek, B.A., 2000. Effect of experimental treatment on housekeeping gene expression: validation by real-time, quantitative RT-PCR. J. Biochem. Biophys. Methods 46 (1–2), 69–81. https://doi.org/10.1016/S0165-022X(00)00129-9.

Shakib, P., Saki, R., Marzban, A., Goudarzi, G., Ghotekar, S., Cheraghipour, K., Zolfaghari, M., 2023. Antibacterial effects of nanocomposites on efflux pump expression and biofilm production in Pseudomonas aeruginosa: a systematic review. Curr. Pharm. Biotechnol. 24, 345–358. https://doi.org/10.2174/1389201024666230412101234.

Silva, A., Silva, V., López, M., Rojo-Bezares, B., Carvalho, J., Castro, A.P., Sáenz, Y., Igrejas, G., Poeta, P., 2023. Antimicrobial resistance, genetic lineages, and biofilm formation in Pseudomonas aeruginosa isolated from human infections: an emerging one health concern. Antibiotics 12, 1248. https://doi.org/10.3390/antibiotics12081248.

Ugwuanyi, F.C., Ajayi, A., Ojo, D., Adeleye, A., Smith, S., 2021. Evaluation of efflux pump activity and biofilm formation in multidrug-resistant Pseudomonas aeruginosa isolated from a federal medical center in Nigeria. Ann. Clin. Microbiol. Antimicrob. 20 (9). https://doi.org/10.1186/s12941-021-00417-y.

Vandesompele, J., De Preter, K., Pattyn, F., Poppe, B., Van Roy, N., De Paepe, A., Speleman, F., 2002. Accurate normalization of real-time quantitative RT-PCR data by geometric averaging of multiple internal control genes. Genome Biol. 3 (7). https://doi.org/10.1186/gb-2002-3-7-research0034 research0034.1.

Venkatesan, M., Fruci, M., Verellen, L.A., Skarina, T., Mesa, N., Flick, R., Pham, C., Mahadevan, R., Stogios, P.J., Savchenko, A., 2023. Molecular mechanism of plasmid-borne resistance to sulfonamide antibiotics. Nat. Commun. 14 (1), 4031. https://doi.org/10.1038/s41467-023-39778-7.

Wahyudi, D., Aman, A.T., Handayani, N.S.N., Soetarto, E.S., 2019. Differences among clinical isolates of *Pseudomonas aeruginosa* in their capability of forming biofilms and their susceptibility to antibiotics. Biodivers. J. Biol. Divers. 20 (5), 1450–1456. https://doi.org/10.13057/biodiv/d200538.

Weimann, A., Dinan, A.M., Ruis, C., Bernut, A., Pont, S., Brown, K., Ryan, J., Santos, L., Ellison, L., Ukor, E., Pandurangan, A.P., Krokowski, S., Blundell, T.L., Welch, M., Blane, B., Judge, K., Bousfield, R., Brown, N., Bryant, J.M., Floto, R.A., 2024. Evolution and host-specific adaptation of *Pseudomonas aeruginosa*. Science 385 (6704). https://doi.org/10.1126/science.adi0908.

Williams, D., Evans, B., Haldenby, S., Walshaw, M.J., Brockhurst, M.A., Winstanley, C., Paterson, S., 2015. Divergent, coexisting *Pseudomonas aeruginosa* lineages in chronic cystic fibrosis lung infections. Am. J. Respir. Crit. Care Med. 191 (7), 775–785. https://doi.org/10.1164/rccm.201409-1646OC.